

CREEP CORRECTION METHOD FOR FORCE APPLICATIONS

J. Sander¹, R. Kumme², F. Tegtmeier³

Physikalisch-Technische Bundesanstalt (PTB), Bundesallee 100, 38116 Braunschweig, Germany

¹jonas.sander@ptb.de, ²rolf.kumme@ptb.de, ³falk.tegtmeier@ptb.de

Abstract:

This paper investigates the creep behaviour of a force transducer at different load levels. Using the results of fast-loading and creep tests, it presents a method for determining a creep correction factor. For this purpose, creep models based on exponentially decaying functions were applied along with an iterative algorithm that takes account of the history of the force-time profile.

Keywords: force transducer; creep; creep correction; continuous force; force applications

1. INTRODUCTION

State of the art in the calibration of force transducers is a procedure defined by ISO 376:2011 [1]. This standard specifies the application of several static load steps to the transducer. With regard to the time-dependent behaviour in the form of creep, however, it merely specifies that an estimate be made, and this only in the range of 30 s to 300 s after loading. Based on [2], [3] and [4], this paper proposes a method for determining a creep correction factor that is particularly suitable for continuous force measurements with rated force-time profiles covering less than one minute.

2. PARAMETER ESTIMATION

A force transducer (Figure 1) with a design similar to that of a material test probe and intended for tests performed to certain dynamic test standards was developed within the EMPIR 18SIB08 project at the University of Stuttgart and PTB Braunschweig [5]. This special transducer with a capacity of 20 kN was used for the investigation described below. The first step was to calibrate the transducer statically according to ISO 376:2011 using a DMP 40 carrier frequency amplifier from HBM with a filter setting of 0.1 Hz Bessel in the compression mode.

Table 1 shows that this force transducer has quite significant zero error, creep and hysteresis, and therefore does not receive a classification under ISO 376:2011 criteria. It is important to note that the creep behaviour exerts a significant influence on the other two criteria. To describe this behaviour and

enable a correction, a new calibration procedure is required. For this purpose, the force transducer was calibrated in a deadweight machine according to the procedure presented in Figure 2. Instead of incrementally increasing static load steps as described in ISO 376:2011, the new procedure uses fast loadings as described in DKD 3-9 Annex 3.1. The force transducer is calibrated in three rotational mounting positions. The signal from the force transducer must be continuously recorded throughout the entire measurement procedure. The reading for each force level is then taken immediately after the signal has stabilised. The repeatability is determined using the measurement series R1 and R2. The mean value X_f for each force level is determined from measurement series R1, R3 and R4, and these are used to determine the reproducibility (also called rotation).

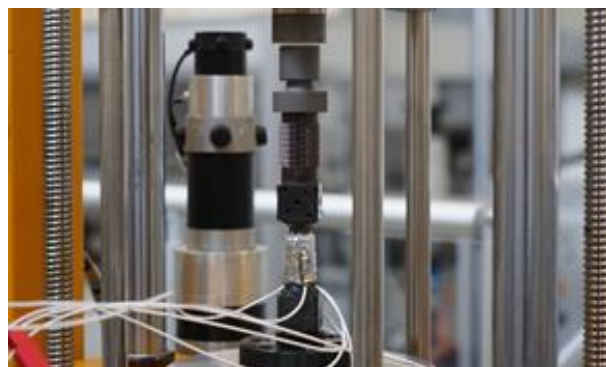


Figure 1: Investigated force transducer with mounting parts for static calibration in 20 kN FSM at PTB Braunschweig

Table 1: Results for the calibration according to ISO 376

Force / kN	Rot. b / %	Rep. b' / %	Zero f_0 / %	Creep c_{Load} / %	Hys. v / %	Interp. f_c / %
2	0.081	0.040	0.206	0.214	1.251	0.070
4	0.119	0.031			0.674	0.008
6	0.118	0.027			0.473	-0.004
8	0.127	0.023			0.351	-0.006
10	0.135	0.015			0.271	-0.006
12	0.135	0.015			0.213	-0.001
14	0.143	0.015			0.163	0.002
16	0.151	0.006			0.112	0.003
18	0.154	0.012			0.063	0.002
20	0.171	0.008				-0.003

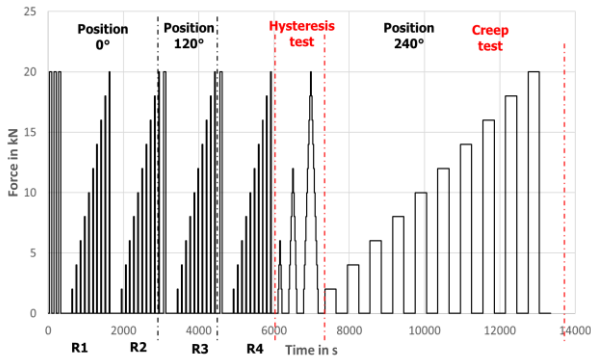


Figure 2: Measurement and validation procedure for determining a user function for a force transducer with creep correction

While the characteristic curve of the force transducer, according to ISO 376:2011, is determined by plotting signal over force, the inverse function (force as a function of the signal), is used in the actual application. That is why the characteristic curve $F_{A_{3,f}}$, which describes the instantaneous indicated force after force application, is then determined from the mean values X_f of the fast-loading series using a third-degree polynomial.

$$F_{A_{3,f}} = A \cdot X_f + B \cdot X_f^2 + C \cdot X_f^3 \quad (1)$$

These four increasing-load measurements series are followed by a hysteresis test in the last installation position. Here, the force is applied in steps with holding times of 30 s per force level up to 30 %, 60 % and 100 % of the full-scale output (FSO). Finally, creep measurements are made with holding times of 300 s, each in 10 % steps from 10 % to 100 % of FSO. All of these measurements were done using a DC voltage amplifier from Dewetron with the DAQP Bridge card with a set sampling rate of 1 kHz and a low-pass filter of 300 kHz. This amplifier made it possible to rule out any filter influence on creep behaviour as well as any delay in the fast-loading measurements. The results of the fast-loading measurements are shown in Table 2, which includes the measured values for rotation, repeatability, and interpolation error. This table also indicates a resolution, which is calculated from the signal-to-noise ratio of the amplifier. Compared to ISO 376:2011 calibration, the reproducibility is slightly improved while the repeatability is comparable.

Creep curves of loading creep and unloading creep are shown in Figure 3 and Figure 4.

A correlation between load and creep can be clearly seen here. The relative creep curves in Figure 5 and Figure 6 show that the 10 % and 100 % creep curves differ in terms of the relative amplitude from the rest, indicating that there is no clean linear dependence between the absolute amplitudes and

the force. The creep models were formed according to equation (2) [6] for the relative creep behaviour.

Table 2: Results for the fast-loading calibration

Force / kN	Rot. b / %	Rep. b' / %	Res. r / %	Interp. f_c / %
2	0.183	0.002	0.074	0.032
4	0.083	0.030	0.039	-0.052
6	0.053	0.008	0.026	-0.010
8	0.062	0.045	0.018	0.001
10	0.071	0.001	0.016	0.049
12	0.051	0.023	0.013	0.008
14	0.037	0.035	0.012	-0.014
16	0.053	0.028	0.010	-0.020
18	0.048	0.010	0.008	-0.010
20	0.071	0.002	0.008	0.015

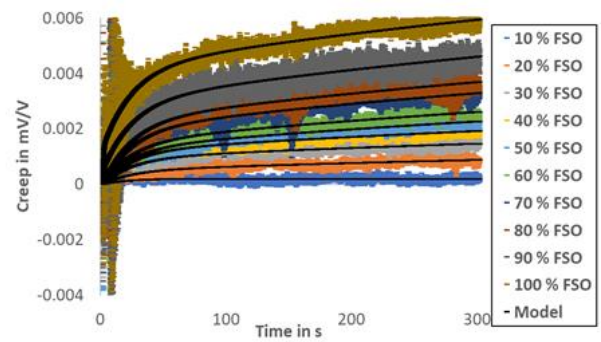


Figure 3: Absolute loading creep after application of load at different load levels from 10 % to 100 % FSO

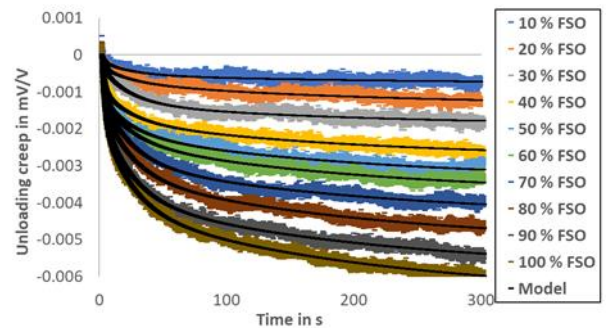


Figure 4: Absolute unloading creep after removal of load at different load levels from 10 % to 100 % FSO

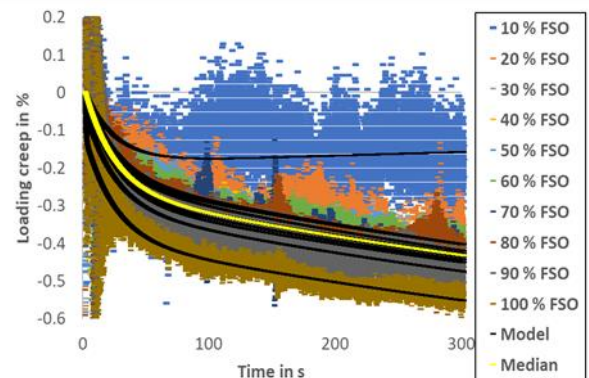


Figure 5: Relative loading creep after application of load at different load levels from 10 % to 100 % FSO

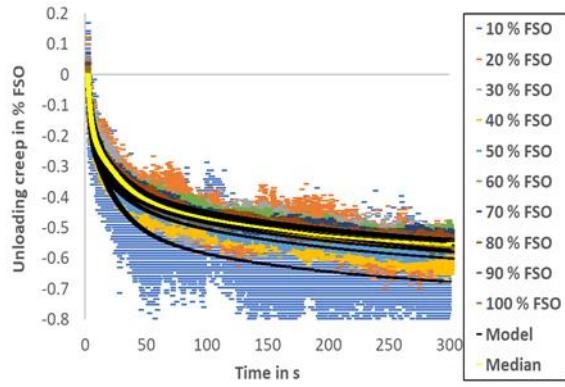


Figure 6: Relative unloading creep after removal of load at different load levels from 10 % to 100 % FSO

$$F_{\text{creep,rel}}(t) = \sum_{k=1}^{k=3} a_k \cdot \left(1 - e^{-\frac{t}{\tau_k}}\right) \quad (2)$$

The time constants τ_k are the same for each model, and the reference value for the calculation of the relative amplitudes a_k for the respective force level is estimated analogously to the fast-loading series.

The parameters determined in this way for loading creep are shown in Table 3 and for unloading creep in Table 4. To simplify the following correction algorithm, the median was formed from the amplitudes for both the loading and the unloading creep with the time constants remaining the same.

3. CORRECTION METHOD

In order to correct for creep behaviour during a certain force-time profile, the creep error $\delta x_{\text{creep}}(t_i)$ must be subtracted from the force value

$F_{A_{3,\text{raw}}}(t_i)$ of the transducer in each time step to yield a corrected force value $F_{A_{3,\text{cor}}}(t_i)$. This error is calculated iteratively taking account of the previous history according to equation (3) [4] which here uses the parameters of the median creep models.

$$\delta x_{\text{creep}}(t_i) = \sum_{k=1}^{k=3} a_k \left[F_{A_{3,\text{cor}}}(t_{i-1}) - e^{-\frac{t_i}{\tau_k}} \sum_{j=0}^{i-1} \left(F_{A_{3,\text{cor}}}(t_j) - F_{A_{3,\text{cor}}}(t_{j-1}) \right) e^{\frac{t_j}{\tau_k}} \right] \quad (3)$$

with: $F_{A_{3,\text{cor}}}(t_0) = F_{A_{3,\text{raw}}}(t_0)$

Figure 7 shows the deviations between the readings of the force transducer using the calibration function from (1) and the reference force generated by the force standard machine during the hysteresis test from Figure 2. It further includes the creep error determined using the correction algorithm and provides a very good description of the observed deviations associated with both increasing and decreasing force levels. The zero error between the different measurement series is also very well depicted in the graph. Only in the last cycle does the determined creep error deviate further from the real data. This is primarily because the deviations of the amplitudes from the median accumulate and may result in a larger error.

Table 3: Parameters of loading creep behaviour at different force levels

Parameters	Creep 10 %	Creep 20 %	Creep 30 %	Creep 40 %	Creep 50 %	Creep 60 %	Creep 70 %	Creep 80 %	Creep 90 %	Creep 100 %	Creep Median
$a_1 / \%$	-0.011	-0.295	-0.256	-0.290	-0.306	-0.283	-0.278	-0.264	-0.277	-0.271	-0.277
$a_2 / \%$	0.008	-0.175	-0.244	-0.188	-0.170	-0.173	-0.220	-0.216	-0.192	-0.192	-0.190
$a_3 / \%$	-0.403	-0.060	-0.043	-0.131	-0.101	-0.084	-0.038	-0.053	-0.094	-0.127	-0.089
τ_1 / s	319.43	319.43	319.43	319.43	319.43	319.43	319.43	319.43	319.43	319.43	319.43
τ_2 / s	32.06	32.06	32.06	32.06	32.06	32.06	32.06	32.06	32.06	32.06	32.06
τ_3 / s	5.00	5.00	5.00	5.00	5.00	5.00	5.00	5.00	5.00	5.00	5.00

Table 4: Parameters of unloading creep behaviour from different force levels

Parameters	Unload Creep 10 %	Unload Creep 20 %	Unload Creep 30 %	Unload Creep 40 %	Unload Creep 50 %	Unload Creep 60 %	Unload Creep 70 %	Unload Creep 80 %	Unload Creep 90 %	Unload Creep 100 %	Unload Creep Median
$a_1 / \%$	-0.239	-0.323	-0.180	-0.273	-0.261	-0.243	-0.196	-0.225	-0.214	-0.236	-0.237
$a_2 / \%$	-0.262	-0.175	-0.267	-0.149	-0.153	-0.162	-0.224	-0.207	-0.208	-0.201	-0.204
$a_3 / \%$	-0.247	-0.158	-0.146	-0.242	-0.212	-0.175	-0.144	-0.155	-0.176	-0.169	-0.172
τ_1 / s	319.43	319.43	319.43	319.43	319.43	319.43	319.43	319.43	319.43	319.43	319.43
τ_2 / s	32.06	32.06	32.06	32.06	32.06	32.06	32.06	32.06	32.06	32.06	32.06
τ_3 / s	5.00	5.00	5.00	5.00	5.00	5.00	5.00	5.00	5.00	5.00	5.00

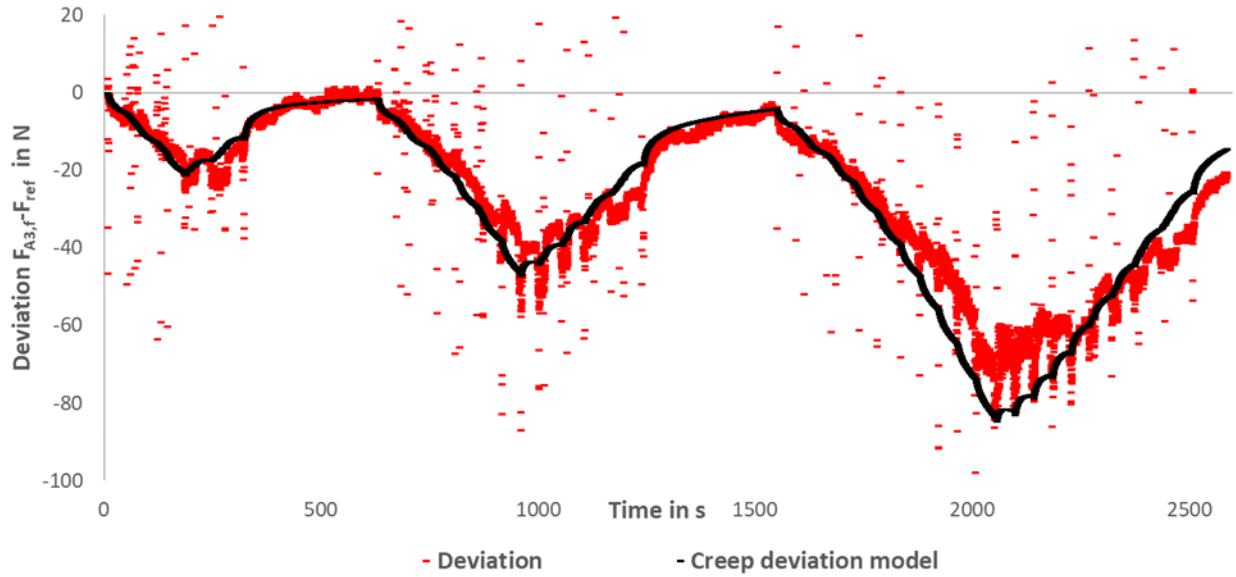


Figure 7: Deviation between force transducer with fast-loading user function $F_{A3,f}$ and reference force of the deadweight machine F_{ref} during hysteresis test (red dots). Modelled creep deviation δx_{creep} (black line) during hysteresis test

Furthermore, the force-time profile of the last cycle clearly exceeds the creep test duration of 300 s, transcending the limits in which the creep models remain valid. Temperature fluctuations can also lead to deviations [7], [8]. In addition, the creep measurement procedure may have produced corrupted creep curves due to excessively short pauses between the measurements. Beyond this, hysteresis effects not resulting from creep can also have a significant impact here.

For the model description of the force transducer with its associated uncertainty, a product model as shown in equation (4) can be used.

$$F_{A3,f}(t_i) = F_{ref} \cdot \prod_{i=1}^n K_i \quad (4)$$

As an example, the correction factor for creep is shown in equation (5).

$$K_{creep} = \left(1 - \frac{\delta x_{creep}(t_i)}{F_{A3,raw}(t_i)}\right) \quad (5)$$

To determine the uncertainty, the hysteresis test is first corrected for creep and then the hysteresis is determined in accordance with ISO 376:2011. The difference between uncorrected hysteresis and corrected hysteresis can be clearly seen in Figure 8 and Table 5. The zero error f_0 is reduced from 0.34 % to 0.04 %. In this case, modelling and further correction of the hysteresis are not possible.

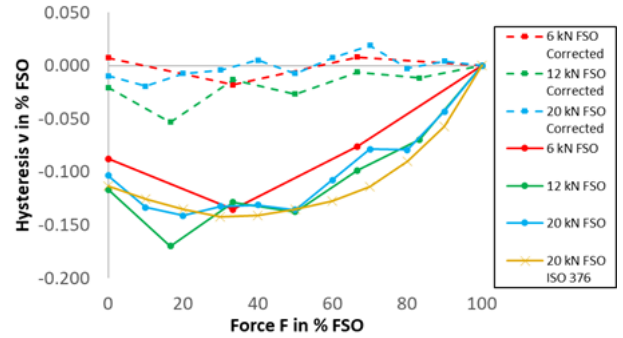


Figure 8: Relative hysteresis vs. applied level of FSO

Table 5: Comparison of creep corrected hysteresis and uncorrected hysteresis

Force / kN	v _{30,corr} / %	v _{60,corr} / %	v _{100,corr} / %	v ₃₀ / %	v ₆₀ / %	v ₁₀₀ / %
2	-0.054	-0.319	-0.194	-0.405	-1.014	-1.342
4	0.012	-0.040	-0.038	-0.114	-0.386	-0.702
6		-0.054	-0.015		-0.275	-0.429
8		-0.009	0.013		-0.148	-0.327
10		-0.014	-0.015		-0.083	-0.269
12			0.012			-0.171
14			0.027			-0.113
16			-0.004			-0.098
18			0.004			-0.048
20						

The expanded uncertainty for each force step i is thus calculated based on ISO 376:2011 as specified in equation (6).

$$W_i(t) = k \cdot \sqrt{\sum_{j=1}^{j=n} w_{i,j}^2 + w_{i,creep-cor}^2(t)} \quad (6)$$

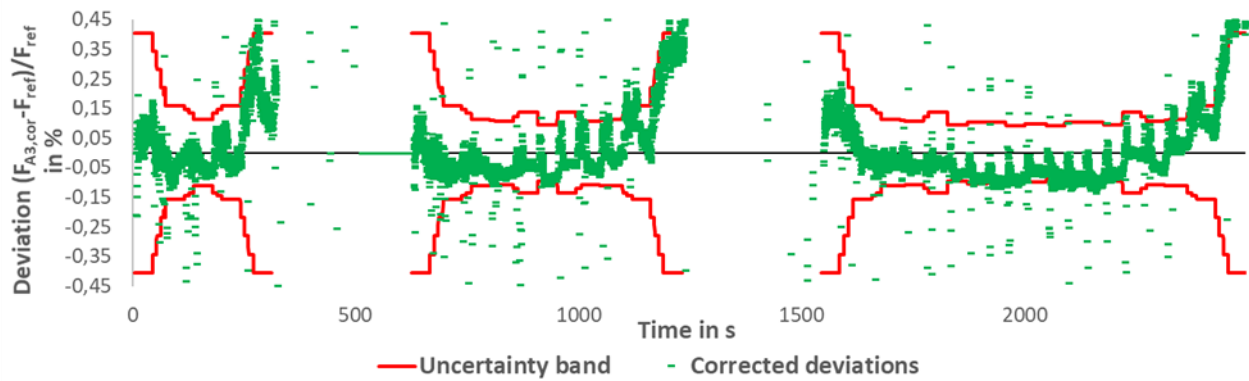


Figure 9: Relative deviation between force transducer with creep corrected user function $F_{A_{3,cor}}$ and reference force of the deadweight machine F_{ref} during hysteresis test

However, due to the reasons mentioned above, it has not yet been possible to estimate the uncertainty contribution $w_{i,creep-cor}(t)$ for this transducer. Figure 9 shows the relative deviations of the corrected data and the reference force of the deadweight machine during the hysteresis test. It can be seen that these deviations are mostly within the extended uncertainty calculated previously without the uncertainty contribution of the correction. Nevertheless, it can also be seen that at the end of each cycle the deviations move slightly outside the uncertainty band. Therefore, an indication of the uncertainty is necessary that includes a specification of temporal and temperature validity limits of the creep correction. However, further investigations are needed for this.

4. SUMMARY

As a supplement to static calibration techniques, a method for determining a creep correction factor is proposed. This factor corrects for creep in each time step taking account of the history of the force-time profile. Using a force transducer specifically developed for use in dynamic test stands, it was possible to show that this correction method can significantly decrease the impact of creep on static measurement results. However, to determine an uncertainty contribution for the correction, the measurement procedure needs to be optimised with regard to the pauses between the creep measurements. In addition, more investigations are needed to determine validation limits for the proposed correction method.

5. ACKNOWLEDGMENT

This work is part of the 18SIB08 project funded by the EMPIR programme.



6. REFERENCES

- [1] ISO 376, "Metallic materials – Calibration of force-proving instruments used for the verification of uniaxial testing machines", 2011.
- [2] DKD-R 3-9, "Continuous calibration of force transducers according to the comparison method", 2018.
- [3] A. Brüge, "Fast Torque Calibrations Using Continuous Procedures", Proc. of IMEKO TC3 Conf., Celle, Germany, 2002. Online [Accessed 20230108] <https://www.imeko.org/publications/tc3-2002/IMEKO-TC3-2002-016.pdf>
- [4] K. L. Phan, "Methods to correct for creep in elastomer-based sensors", IEEE Sensors Conference, Lecce, Italy, 26-29 October 2008, pp. 1119-1122. DOI: [10.1109/ICSENS.2008.4716637](https://doi.org/10.1109/ICSENS.2008.4716637)
- [5] A. Nitschke, S. Neumann, S. Gerber, R. Kümme, F. Tegtmeyer, "Development of a force transfer standard for the calibration of cyclical forces in materials testing machines with quantification of parasitic factors", Proc. of Sensoren und Messsysteme 2022, Nuremberg, May 2022.
- [6] R. Mitchell, S. Baker, "Characterizing the Creep Response of Load Cells", VDI-Berichte 312, 1978, pp. 43-48.
- [7] T. Bartel, S. Yaniv, "Creep and Creep Recovery Response of Load cells Tested According to U.S. and International Evaluation Procedures", Journal of Research of the National Institute of Standards and Technology, vol. 102, 1997, no. 349.
- [8] M. Kühnel, "Traceable measurement of the mechanical properties of spring elements for the force measurement technology" (in German), PhD thesis at the University of Ilmenau, 2013.